DOI: 10.13009/EUCASS2019-495

STUDY OF THE SHIELDING PERFORMANCE OF WHIPPLE SHIELD ENHANCED BY IMPEDANCE-GRADED MATERIALS

Pinliang Zhang, Zizheng Gong**, Dongbo Tian, Guangming Song, Qiang Wu, Yan Cao, Ming Li*

**Beijing Institute of Spacecraft Environment Engineering, Beijing 100094, China*

e-mail: zhangpinliang620@126.com

*** Beijing Institute of Spacecraft Environment Engineering, Beijing 100094, China*

e-mail: gongzz@263.net

Abstract

An improved Meteoroids and Orbital Debris shielding structure for spacecraft is presented, using a bumper constructed from impedance-graded materials. The shielding performance of a shield enhanced by Ti-Al-nylon impedance-graded materials are investigated experimentally, using a two-stage light gas gun at velocities of 3.50 and 6.50 km/s, the critical diameter and ballistic limit curve are obtained. The results show that the shielding capability of a Ti-Al-nylon shield is greater than that of an aluminum Whipple shield and Al-Mg shield where the bumper has the same areal density. A theoretical analysis and numerical simulation are performed to explore why Ti-Al-nylon shields achieve a better shielding performance.

1. Introduction

It is well established that hypervelocity impacts of Meteoroids and Orbital Debris (M/OD) can significantly affect the performance and even integrity of spacecraft. However, the amount of space debris has increased significantly. In order to successfully defend such high speed impact loadings, a lightweight and long-duration flight dual-wall Whipple shield have been proposed [1]. The Whipple suggested that a thin “bumper” placed in front of the pressure hull, would obviously increase the spacecraft’s level of protection against impacting objects. From Apollo to the International Space Station, the Whipple shield concept has provided the baseline for shielding against the impact of Meteoroids and Orbital Debris [2].

Many improved or enhanced shield configurations have been proposed and tested to deal with these threats based on the Whipple shield up to now [3-6]. However, all of them use an initial sacrificial sheet or bumper to initiates fragmentation, melt and vaporize an impacting object that expands over a void before hitting a subsequent shield wall of a critical component. It is believed that the bumper is the key element because it determines the projectile fragments after initial impact [7].

In previous work, an enhanced Whipple shield is presented that employs a thin impedance-graded material (IGM) bumper to replace the homogeneous single-layer bumper. IGM is an impedance-mismatched multilayering of materials. Preliminary hypervelocity impact tests were carried out to study the shielding performance of Al-Mg and Ti-Al-nylon IGM shields[8, 9]. Some positive indications suggested that the IGM shields is more effective in fragmenting projectiles and dissipating

DOI: 10.13009/EUCASS2019-495

energy. It was preliminarily observed that the IGM enhanced shield can improve the shielding performance compared with an aluminum Whipple shield.

In this paper, a series of hypervelocity impact tests are carried out to compare the ballistic limit of a shield enhanced with a Ti-Al-nylon bumper with that of Al-Mg and aluminum Whipple shields with the same areal density. Furthermore, the excellent performance of IGM shielding material is proved.

2. Experiments

All of the metallic impedance-graded bumpers prepared via accumulative roll bonding, and the metal and nylon layers were glued together with a two-component epoxy adhesive.

In order to reveal the maximum protection capability of Ti-Al-nylon shields, six new successful normal incidence impact tests for the Ti-Al-nylon shields by Al-2A12 aluminum spheres were carried out on a two-stage light-gas gun at impact velocities of approximately 3.5 and 6.5 km/s. A 0.20/0.27/1.00 mm thick Ti/Al/nylon IGM bumper, which replaced an aluminum bumper and was mounted in front of an Al-5A06 rear wall (300 mm×300 mm). The areal density of bumper (AD=0.279 g/cm^2), shield spacing (S =100 mm) and thickness of the rear wall (t_w=2.5 mm) were constant. Experimental schematic diagram was shown in Fig.1 of Ref. [8]. Failure was defined as the ejection of any material from the rear surface of the rear wall (i.e., detached spall) or clearly perforated. The critical state is defined as exhibiting a spall blister with a single crack or a system of cracks in the rear surface of the rear wall. The experimental configurations are summarized in Table 1.

Table 1 Experimental conditions, shield parameters, normalized hole diameter d_h/D_p and shields status after impact.

Expt. No.	Projectile			Shield		
	Materials	D_p[a] (mm)	V[b] (km/s)	Bumper materials	t_b[c] (mm)	Pass/ Fail
1	Al	3.50	3.55	Ti-Al-nylon	1.47	Pass[8]
2	Al	3.75	3.54	Ti-Al-nylon	1.47	Critical
3	Al	4.00	3.56	Ti-Al-nylon	1.47	Fail
4	Al	5.00	6.40	Ti-Al-nylon	1.47	Pass[8]
5	Al	5.25	6.52	Ti-Al-nylon	1.47	Fail
6	Al	5.50	6.27	Ti-Al-nylon	1.47	Fail

[a] represents the diameter of projectile.

[b] represents the impact velocity.

[c] represents the thickness of bumper.

3. Results

Views of the damage patterns produced on the rear walls of Expt.1 and Expt.4 are shown in Fig.7 and Fig. 5 in Ref. [8], respectively. For Expt.1, there are few craters concentrated in the center region of the rear wall, most of the larger projectile fragments distributed in a quasi-circular shape around the edge of the center damage area, it is a pass state. The Ti-Al-nylon shields achieved an undisputed “pass state" for Expt.4.

Expt.2 indicates that a 3.75-mm-diameter projectile impacting at 3.54 km/s cause critical to an assessment of performance of the shield. Two perforations on the rear walls for Expt.3 indicate obvious

DOI: 10.13009/EUCASS2019-495

failures. On the contrast, the rear wall for Expt.1 did not fail but slight bulge. When the projectile diameter increased to 5.25 mm at 6.52 km/s in Expt.5, shield was in a failure state, and the rear wall of the full-scale shield exhibited progressively larger regions of tearing damage rather than detached spall or pinhole-sized perforations as the projectile diameters increased according to Expt.6.

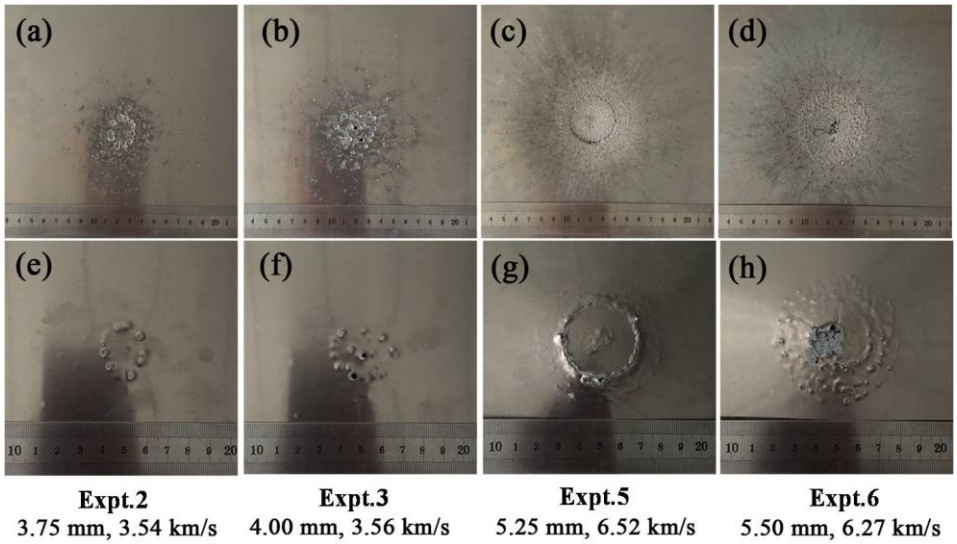

Fig. 1 Views of the damage patterns produced on the rear walls. (a) (e) correspond to Expt.2, (b) (f) correspond to Expt.3, (c) (g) correspond to Expt.5 and (d)(h) correspond to Expt.6.

Performance data for all tests using Ti-Al-nylon shields are compared with the aluminum shields in Fig. 2. The ballistic limit curve of aluminum shields were obtained experimental in preliminary study, and described in detail in the Ref. [9]. The ballistic limit curve (BLC) were fitted by using the least square method. It can be seen that the critical projectile diameter for Ti-Al-nylon shields sharply increases in contrast with the aluminum shields. The critical projectile diameter for Ti-Al-nylon shield is 5.14 mm at about 6.50 km/s, it is improved about 38.2 % contrast with aluminum shields 3.72 mm. The critical projectile diameter for Ti-Al-nylon shield is 3.43 mm at about 3.50 km/s, it is improved about 21.2 % contrast with aluminum shields 2.83 mm.

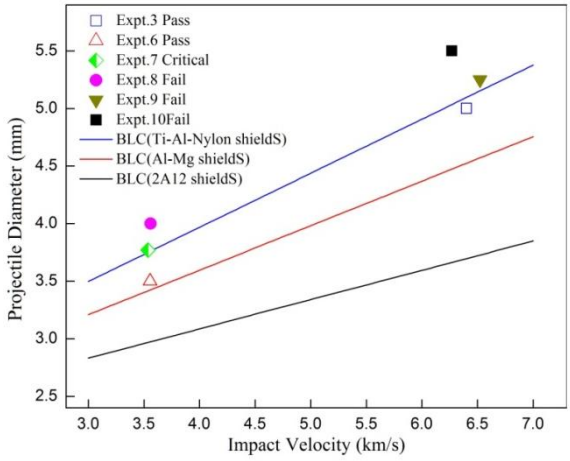

Fig. 2 Ballistic limit curves and test data for Ti-Al-nylon shields and compare with conventional aluminum and Al-Mg Whipple shields.

To reveal the shielding performance of the Ti-Al-nylon impedance-graded- material-enhanced Whipple shield, the BLC of Al/Mg shields[9] are shown in Fig.2. It can be seen that the critical projectile diameter for Ti-Al-nylon shields sharply increases in contrast with the Al-Mg shields.

DOI: 10.13009/EUCASS2019-495

4. Analysis and discussion

4.1 Strength of a shockwaves

There is reasonably compelling evidence that the strength of a shockwaves is largely responsible for fragmentation of projectiles[10-12]. The strength of a shockwaves P_H can be obtained based on shockwave theory and the impedance matching method, and is given by

$$P_H = \rho_{01}(C_{01}u_{p1} + \lambda_1 u_{p1}^2) \tag{1}$$

where u_p is the particle velocity; ρ_0 and C_0 are the density and sound speed in the material at zero pressure, respectively; λ is the coefficient in the Rankine-Hugoniot relationship; and the subscript "1" represents the projectile. The calculation process is described in detail by Meyers [13]. Table 2 presents the parameters of materials. The parameters from Ref. [8, 9]. C_0 is the sound speed, λ is the coefficients in the Rankine-Hugoniot relationship, and γ_0 is the Grüneisen parameter (at 0 GPa).

Table 2 The key properties of materials

Material	Density (g/cm^3)	C_0 (km/s)	λ	γ_0	Melting temperature (℃)	Vaporization Temperature (℃)
Ti6Al4V	4.419	5.130	1.028	1.23	1800	3000
Al2024-T4	2.785	5.328	1.338	2.00	660	2057
AZ31B	1.776	4.516	1.256	1.43	651	1107
PA66	1.140	3.890	1.180	0.87	260	350[a]

[a] decomposition temperature for polymer

The calculation results of impact velocity at 6.5 km/s are listed in Table 3. It suggest that either the aluminum bumper or the Al-Mg bumper is an aluminum-on-aluminum impact event, thus producing equal pressure. The calculated peek shock pressure was approximately 86.6 GPa for aluminum and Al-Mg bumper at an impact velocity of 6.5 km/s. However, for Ti-Al-nylon bumper, it is an aluminum-on-titanium impact event, high impedance titanium pushes the aluminum projectile to a much higher pressure, the peek shock pressure was approximately 102.7 GPa.

4.2 Wave characterization

Unlike a homogeneous single-layer bumper, the IGM bumper is a multi-layer structure, and thus the wave propagation in this structure is different. After a projectile impacts an IGM bumper, two shockwaves (S1, S2) are generated in opposite directions at the same time. When a shockwave moving through the bumper meets an interface with a new material, the shock is transmitted at a different strength into the target material, and a new wave is reflected back. As a shockwave passes through a material interface into a region of lower acoustic impedance, a transmitted shockwave and reflected rarefaction are both generated. Therefore, for a multi-layer bumper a series of reflected rarefactions are generated, which propagate into the projectile. When a transmission shockwave reaches the free surface of a bumper or projectile, it is also reflected as a rarefaction wave. As these rarefaction waves interact, regions of tension form. If the net tension stress exceeds the material strength, then a fracture will occur. A fracture of the projectile or target can be interpreted as a multiple-spalling phenomenon[8,9]. That is more layers or more rarefaction wave reflection behavior, the smaller

materials fragments are produced. Therefore, Ti-Al-nylon bumper has more efficient projectile damage ability than Al/Mg bumper, due to its more layers of structure.

On the other hand, it can be seen that compared with monolithic Al-2A12 bumper, the propagation time of shock wave in bumpers increase sharply for IGM bumper at the same impact velocity, especially for Ti-Al-nylon bumper (Table 3). In this case, the rear part of projectile have enough time to get very hot.

Table 3 Calculation results[8,9] [a]

Bumper		2A12	Al-Mg	Ti-Al-nylon
Shock wave strength (GPa)		86.5	86.5	102.7
Propagation time(μs)		0.105	0.136	0.163
Residual internal energy (MJ/kg)	Projectile	0.941	0.941	1.218
	Bumper	0.941	L1:0.941 L2:1.677	L1:0.766 L2:0.951 L3:2.822

[a] L1, L2 and L3 represent the sequence number of IGM layer from impact side.

The numerical simulation of projectile hypervelocity impact on bumpers have been carried out using hydro-codes. The parameters used in calculation are list in Table 2. The shock process in the projectile of IGM bumper, and compared to Al-2A12 bumper are graphically represented in Fig. 3. The shock wave strength producted by hydro-codes as the same as the results in Table 3. It can be seen that the duration of shock wave for IGM bumper is longer than monolithic Al-2A12 bumper. The plateaus which is related to a rarefaction wave overtake the shock wave in projectile are appeared in shock process profile. There are one and two plateaus for Al-Mg and Ti-Al-nylon bumper, accroding to one and two materials interface, respectively. This proves the calculation results and analysis in this paper.

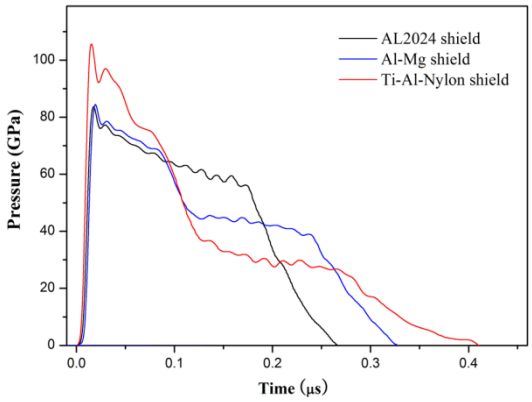

Fig. 3 The calculated shock process in the projectile of Al-2A12, Al-Mg and Ti-Al-nylon shield

4.3 Thermodynamic states

It is considered that the heating effects are important in determining the size of particles in the debris cloud. The specific internal energy are calculated based on Rankine-Hugoniot relationship and Mie-Grüneisen EOS, and detailed in the Ref. [14]. In our calculation, Mie-Grüneisen EOS is only using to demonstrate the magnitude of residual energy and temperature rise of materials, assume that no vaporization of material would take place. It should be noted that the contribution of plastic

deformation can be neglected, as the entropy production in non-linear shock compression event plays a key role in material heating [15].

The results of calculation are listed in Table 3. Compared with monolithic Al-2A12 and Al-Mg IGM bumper, the material temperature rise in the projectile are obviously higher at the same impact velocity when Ti-Al-nylon bumper is used, due to the higher acoustic impedance of outer layers. The higher amplitude of shock waves induces more severely heating of the material, so that the strength of the projectile and bumper is degraded more, combined with the low decomposition temperature of nylon leading to vaporization at higher impact velocity. Thus, the particle size of the bubble and the debris cloud rear element that are produced by Ti-Al-nylon bumper is smaller than that produced by Al-2A12 and Al-Mg bumper.

5. Conclusion

In conclusion, some positive indications suggested that the IGM enhanced Whipple shield is more effective in fragmenting projectiles and dissipating energy. The critical projectile diameter for IGM shields sharply increases in contrast with the aluminum shields. The Ti-Al-nylon bumper has the best protection performance in this work (about 38.2% increase compared to conventional aluminum shields with the same bumper areal density). The results of theoretical analysis and numerical simulation showed that the Ti-Al-nylon bumper can generate higher shock pressures and induce higher temperature rises, due to high impedance titanium. In addition, it is found that the IGM bumper alters the wave propagation path and duration time, which leads to sufficient time for materials to become very hot and break up. These tests demonstrate the potential applications of impedance-graded structures in the bumpers of M/OD shields.

References

[1] Whipple FL. Meteorites and space travel. Astron J 1947;52(5):131.

[2] Ryan S, jorkman MB, Christiansen EL. Whipple shield performance in the shatter regime. Int J Impact Eng 2011; 38: 504-510.

[3] Piekutowski AJ, Poormon KL, Christiansen EL, Davis BA. Performance of Whipple shields at impact velocities above 9 km/s. Int J Impact Eng 2011; 38(6): 495–503.

[4] Wu Q, Zhang QM, Long RR, Zhang K, Guo J. Potential space debris shield structure using impact-initiated energetic materials composed of polytetrafluoroethylene and aluminum. Appl Phys Lett 2016; 108: 101903.

[5] Zhang XT, Liu T, Li XG, Jia GH. Hypervelocity impact performance of aluminum egg-box panel enhanced Whipple shield. Acta Astronaut 2016; 119: 48–59.

[6] Christiansen EL. Enhanced meteoroid and orbital debris shielding. Int J Impact Eng 1995; 17: 217–228.

[7] Cour-Palais BG. Hypervelocity impact in metals, glass and composites. Int J Impact Eng 1987; 5(1–4): 221–237.

[8] Zhang PL, Xu KB, Li M, Gong ZZ, Song GM, Wu Q, Cao Y, Tian DB, Yu ZJ. Study of the shielding performance of a Whipple shield enhanced by Ti-Alnylon impedance-graded materials. Int J Impact Eng 2019;124: 23–30.

[9] Zhang PL, Gong ZZ, Tian DB, Song GM, Wu Q, Cao Y, Xu KB, Li M. Comparison of shielding performance of Al/Mg impedance-graded-material enhanced and aluminum Whipple shields.

Int J Impact Eng 2019;126: 101–108.

[10] Grady DE, Kipp ME. Experimental measurement of dynamic failure and fragmentation properties of metals. Int J Solids Struct 1995; 32(17–18): 2779–2781.

[11]Grady DE, Kipp ME. Fragmentation properties of metals. Int J Impact Eng 1997; 20(1–5): 293–308.

[12] Piekutowski AJ, Poormon KL. Impact of thin aluminum sheets with aluminum spheres up to 9 km/s. Int J Impact Eng 2008; 35: 1716–1722.

[13] Meyers MA. Dynamic behavior of materials. New York: John Wiley & Sons; 1994.

[14] Maiden GJ, McMillan AR. An investigation of the protection afforded a spacecraft by a thin shield. AIAA J 1964; 2(11): 1992–1998.

[15] Zhang QM, Tan QM, Zhang DL, Cheng CM. Melting effects of aluminum dualsheet structure in hypervelocity impact. Acta Mechanica Sinica 1995; 27: 257–266.